

An Investigation of PAHs in Meromictic Pink Lake, Gatineau Park, Quebec

By

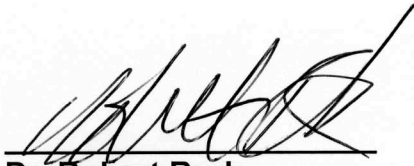
Davin M.R. Carter

**A report submitted to the Department of Chemistry in partial fulfillment of
the requirements for the Degree of Bachelor of
Science with Honours.**

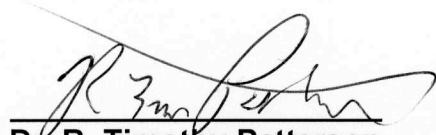
**Carleton University
Department of Chemistry
Ottawa, ON
April 27, 2005**

Statement of Approval

The undersigned hereby recommends to the Department of Chemistry acceptance of this report, submitted by Davin M.R. Carter in partial fulfillment of the requirements for the degree of Bachelor of Science with Honours.



Dr. Robert Burk
Thesis Supervisor
Dept. of Chemistry



Dr. R. Timothy Patterson
Thesis Supervisor
Dept. of Earth Sciences

Abstract:

This interdisciplinary research investigated PAH (polycyclic aromatic hydrocarbon) levels in sediment freeze cores from Pink Lake, Gatineau Park to determine their suitability as proxies for land-use change. PAHs are a class of ubiquitous organic contaminants whose chemical properties make them resistant to environmental degradation. Levels of PAHs in sediment freeze cores from Pink Lake, Gatineau Park, were found to be below instrumental detection limits. Detection limits of the GC-MS for PAHs operated in SIM mode was found to be in the low parts per billion range (nanogram of analyte injected). Sediments from the bottom of meromictic Pink Lake, in Gatineau Park, may still offer a view of historical environments in the annually deposited sediments if larger samples are collected but will require extensive clean-up.

Acknowledgments:

This project was undertaken with the support of both Tim Patterson and Bob Burk. Their willingness to co-supervise me made for a unique learning experience. The time and critical review from both supervisors was valuable.

Advice from Fred Casselman and Tony O'Neil was timely and helpful. The samples and lake measurements were collected by a large field team from Patterson lab, Pisaric lab and Michel Lab of Carleton University.

My wife, Heather, has been endlessly patient and supportive without whom I couldn't have finished my studies at Carleton. I wish to acknowledge my family for giving the opportunity to write this thesis. My mother, Therese, brother Aidan and father Alan, have provided support in many different ways over the years.

This project is dedicated to a great Canadian who was taken, during this research, in a sudden accident September 8, 2004. A close friend and mentor to me, he helped thousands of young Canadians explore careers in math, science and technology. For his contributions to Canadian youth and national unity Bruce MacMillan will always be remembered.

Table of Contents

SUBJECT	PAGE
Abstract	i
Acknowledgements	ii
List of Tables, Figures and Plates	iv
1. INTRODUCTION	1
1.1 Polycyclic Aromatic Hydrocarbons	1
1.2 Study Area	3
1.3 Analytical Techniques	6
1.3.1 Extraction	6
1.3.2 Chromatography	7
1.3.3 Gas Chromatography	8
1.3.4 Tailing/Fronting of Chromatographic Peaks	12
1.3.5 Peak Broadening of Chromatographic Peaks	12
1.3.6 van Deemter Equation	14
1.3.7 Mass Spectrometry	15
1.3.8 Ion-Trap Mass Spectrometry	15
1.3.9 Mass Spectra	16
2. EXPERIMENTAL	17
2.1 Sample Collection	17
2.2 X-Ray/Lead Analysis	19
2.3 PAH Analysis	20
3. RESULTS AND DISCUSSION	24
3.1 PAH Analysis of Pink Lake Sediment	24
3.2 GC Temperature Programming	24
3.3 Mass Spectrometry	30
3.4 Sediment Extracts	34
3.5 Sample Clean Up	36
3.6 Pink Lake	39
3.7 Suitability of PAH as Land-Use Change Proxy	42
4. CONCLUSION	43
5. REFERENCES	44

List of Tables, Figures & Plates

NUMBER		PAGE
Table 1	Selected Physical Properties of PAHs	3
Table 2	GC Temperature Program for PAH Analysis	25
Table 3	SIM Program for PAH Analysis	30
Table 4	Water Content of Pink Lake Freeze Core	39
Figure 1	Chemical Structures of EPA Priority PAHs	2
Figure 2	Map of Study Area	4
Figure 3	Various Chromatographic Peak Shapes	12
Figure 4	Peak Broadening due to Multiple Paths	13
Figure 5	Peak Broadening due to Longitudinal Diffusion	13
Figure 6	Peak Broadening due to Mass Transfer	14
Figure 7	Ion-Trap Mass Spectrometer	15
Figure 8	Schematic of Varian Saturn II GC-MS	22
Figure 9	Soxhlet Apparatus	23
Figure 10	Chromatogram and Mass Spectra of No Injection	26
Figure 11	Chromatograms of increasing Column Bleed Effect with Decreasing Analyte Concentration	27
Figure 12	Interference of Column Bleed on Later Eluting PAHs	29
Figure 13	Chromatogram of PAH Mixture using SIM Program	31
Figure 14	Mass Spectra of Selected PAHs	32
Figure 15	Anthracene Analytical Calibration Curve	33
Figure 16	Variety of Colors from Extracts	35
Figure 17	Analyte Extraction into Methanol via a Soxhlet	35
Figure 18	Photo of Samples at Different Stage of Analysis	36
Figure 19	Extract Clean Up via Florisil Columns	37
Figure 20	Chromatograms of Spiked Sediment Extracts Eluted from Florisil Columns with Solvents of Differing Polarity	38
Figure 21	Dependence of Oxygen Levels on Water Depth	40
Figure 22	Dependence of Water Temperature on Water Depth	40
Figure 23	Sub-Bottom Profile of Pink Lake	41
Plate 1	Photographs of Study Site	5
Plate 2	Photographs of Sample Collection	18
Plate 3	Photographs of Stages of Processing	20

1. Introduction:

1.1 Polycyclic Aromatic Hydrocarbons

Polycyclic aromatic hydrocarbons (PAHs) are a class of ubiquitous organic contaminants. PAHs are characterized by fused benzene rings that make PAHs resistant to environmental degradation (Wang, 2001). PAHs can be both natural and anthropogenic in origin forming via several pathways: biosynthesis, pyrogenic and even extraterrestrial (Naraoka, 2000). The chemical structures of PAHs vary widely, as shown in Figure 1, but are generally environmentally stable making them persistent organic pollutants (POPs). Do to their hydrophobic nature (Notar, 2000) PAHs adsorb onto sediments limiting their bio-availability (Wang, 2001).

Background concentrations of individual PAHs have been found to range from 1-10 part per billion (ppb) in various sediments throughout Germany (Wilke, 2000). Total PAH levels in the Fraser River Basin, British Columbia was found to be 100-500 ppb dry w/w from sediment cores (Yunker, 2003). The structure and relative amounts of different PAHs can be used to identify their source in the environment. Alkylated PAHs are found in fossil fuels, while unsubstituted PAHs are formed by high temperature combustion (Mosi, 1998, Wang, 2001).

Levels of PAHs deposited on soils from forest fires have been found to diminish by a factor of four within a year (Kim, 2003). It is hoped that levels of PAHs remain largely constant when deposited on a meromictic lake such as Pink Lake. PAHs from large fires local to the study area in 1875, 1864, 1854, 1780 and 1763 (Cwynar, 1977) may be found in sediments.

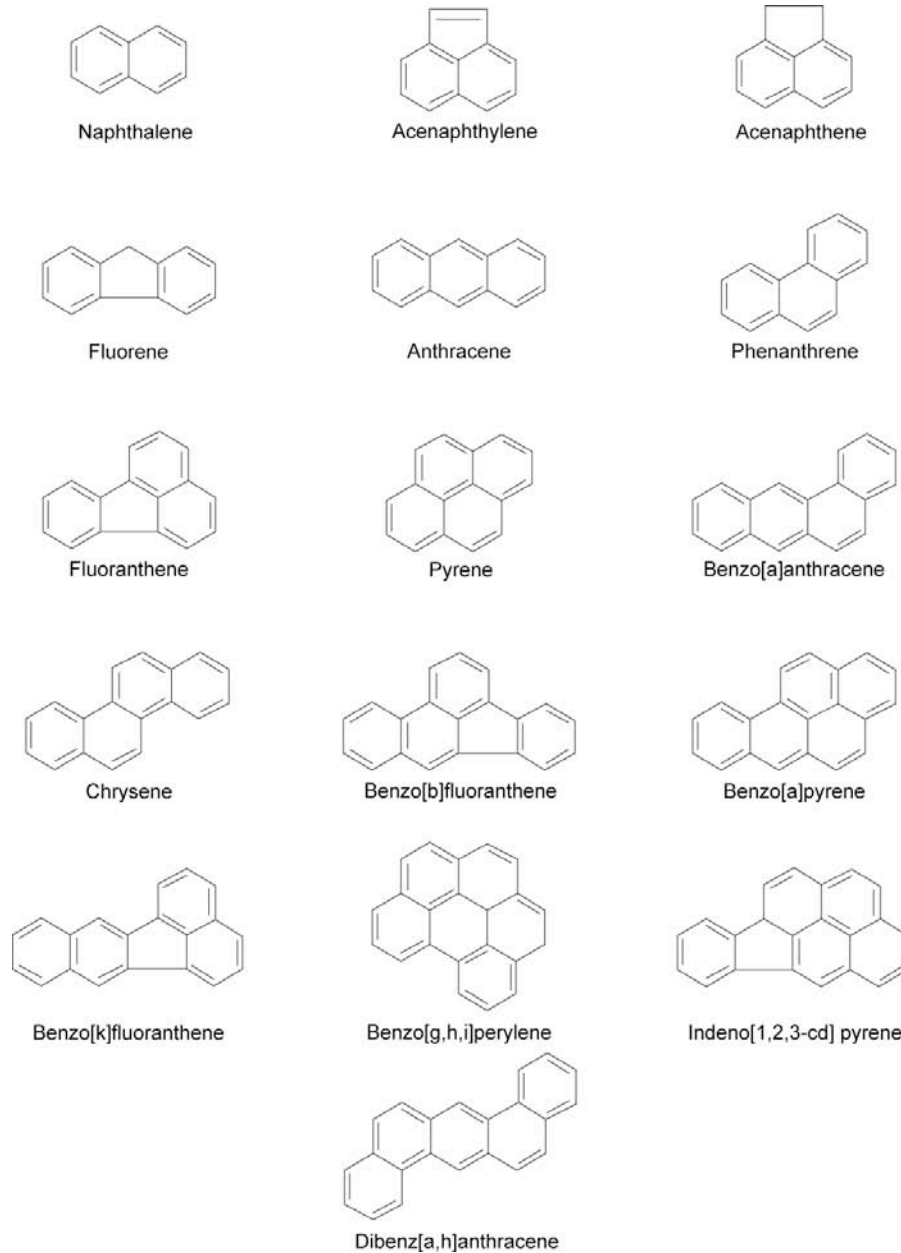


Figure 1: Chemical Structures of EPA Priority PAHs

Physical data on PAHs used in EPA method 610 is given in table 1. Generally heavier compounds have higher melting and boiling points.

Compound	Formula	MW (g)	MP (°C)	BP (°C)
Naphthalene	C ₁₀ H ₈	128	80.6	218.
Acenaphthylene	C ₁₂ H ₈	152	93.5-94.5	265.
Acenaphthene	C ₁₂ H ₁₀	154	95.	279.
Fluorene	C ₁₃ H ₁₀	166	116.	295.
Anthracene	C ₁₄ H ₁₀	178	217.5	340.
Phenanthrene	C ₁₄ H ₁₀	178	99.5	340.
Fluoranthene	C ₁₆ H ₁₀	202	110.8	375.
Pyrene	C ₁₆ H ₁₀	202	156.	404.
Benzo[a]anthracene	C ₁₈ H ₁₂	228	159.8	437.6
Chrysene	C ₁₈ H ₁₂	228	255.8	448.
Benzo[b]fluoranthene	C ₂₀ H ₁₂	252	167.	357.
Benzo[a]pyrene	C ₂₀ H ₁₂	252	176.5	495.
Benzo[k]fluoranthene	C ₂₀ H ₁₂	252	215.7	480.
Benzo[g,h,i]perylene	C ₂₂ H ₁₂	276	278.3	500.
Indeno[1,2,3-cd]pyrene	C ₂₂ H ₁₂	276	162.5	536.
Dibenz[a,h]anthracene	C ₂₂ H ₁₄	278	266.	524.

Table 1: Selected Physical Properties of PAHs (Chemfinder, 2005)

1.2 Study Area

Pink Lake is located in Gatineau Park, Quebec shown in figure 2. Hardwoods that grow on the 30 m cliffs that surround the lake are seen in plate. The area was settled by an Irish family, the Pink's, whose name graces not only the lake but a cemetery and road (NCC, 2005). The lake, 162 m above sea level, thought was inundated by the Champlain Sea 13,000 yr B.P. Isostatic rebound of the area resulted in the lake being isolated from the Sea 11,000 yr B.P.

Transformation of the salt water lake into a fresh water lake has been shown by

fossil analysis to have taken 3,000 years due to the low level of fresh water input (Jones, 1984). The lake is meromictic and oxygen is absent in the bottom of Pink Lake (Dickman, 1978). The lack of organisms in the bottom of the lake means there is likely no bio-degradation of PAHs. The green color of the lake water is due to microscopic algae, to a depth of 15m, causing eutrophication, the process of total oxygen fixation by biological activity (Dickman, 1978). The lake contains a formerly salt-water fish, three spined stickle back (*Gasterosteus aculeatus*), that has adapted to the fresh water of the lake (Mott, 1981).



Figure 2: Map of Study Area



Plate 1: Photographs of Study Site

Calcium carbonate begins to precipitate out of the water column when the water temperature increases and pH increases in the spring (May). The precipitation declines in the fall when temperatures decrease. From the spring to fall decomposing organic matter sequesters oxygen in the water thereby lowering the dissolved oxygen levels. During this period photosynthetic bacteria replace algae as the primary producers. In the late fall, winds cause an oxygen infusion into the anaerobic layer causing a mass die off of the bacteria. It has been reported by Dickman that up to 60% of the annual sediment deposition occurs within 14 days in the fall. The decomposition of the anaerobic bacteria starts cycle over (Dickman, 1978). October sediments were found to contain nearly 90% bacteria, dominated by purple sulfur bacteria (Dickman, 1978). The thick ice cover on the lake up to 400 cm limits the growth of algae and bacteria. This cyclical process has been found in similar lakes such as Crawford Lake and Fayetteville Green Lake (Dickman, 1978).

1.3 Analytical Techniques

Generally, analysis of PAHs in sediments involves: sample collection, sample preparation, analyte extraction, clean up, quantification. Traditional analyte extraction involves transferring the analytes adsorbed onto the sediment to an organic solvent suitable for analysis. Variations on solvent baths such as sonication, shaking or Soxhlet extractors are commonly used (Song, 2002). Analytical methods for PAH are generally well developed, but often need to be optimized for specific samples.

1.3.1 Extraction

In a thorough examination of common extraction methods: mechanical shaking, Soxhlet extraction and ultrasonic extraction, Song et al. found little difference in recoveries of environmental samples. They concluded that sonication with its considerable time savings over shaking and Soxhlet extractions, and use of significantly less solvent compared to Soxhlet extractions, made sonication a more efficient method of analyte extraction (Song, 2002).

Recovery rates have been found to be proportional to the number of aromatic rings of the PAH. Lower mass PAHs like naphthalene, acenaphthene and acenaphthylene have been reported to have low recovery rates, ranging from 40-55%, thought to be due to their higher volatility and higher water solubility than chrysene, benz(a)anthracene, benzo(k)fluoranthene and other higher molecular weight PAHs. High weight PAHs can have extraction coefficients as high as 80-96% (Song, 2002).

Soil moisture was found by Song et al. not to have an effect on extraction efficiency in less polluted (PAH content between 2-25 mg/kg) soils. However water content of heavily contaminated soils (PAH content > 500 mg/kg) was found to affect ultrasonic extraction. The use of more polar solvents like acetone and dichloromethane (1:5) has been found by Song and others to cancel the water effect. (Song, 2002)

1.3.2 Chromatography

Chromatography encompasses the separation of compounds by chemical methods. The origin of chromatography is attributed to Russian scientist Mikhail Tswett in his investigations of chlorophyll pigments in plant leaves. Tswett used a column packed with calcium carbonate to separate plant extracts producing a series of colored bands. Derived from the Greek chromatous (color) and graphein (to write) chromatography has developed into a powerful analytical technique that

can be used to separate complex mixtures into their constituent components.

(Berezkin, 1991, Groß, 1975)

1.3.3 Gas Chromatography

Low molecular weight, non polar, volatile compounds can be analyzed by GC.

Taking advantage of differences in physical properties between chemical compounds, gas chromatography (GC) involves a mobile gas phase and a solid stationary phase. Complex mixtures can be separated based on their interactions with the column, the stronger the interaction between an analyte and the column, the longer it takes the compound to elute from the end of the column. In practice a small volume of sample (typically μL range) is injected into the capillary column (hollow glass tube 20-100 m long), where the mixture interacts with the coating of the column, a polymeric substance (usually a polydimethylsiloxane derivative)

By the “like dissolves like” principle, low to medium polarity compounds can be separated via a low to medium polarity column. A DB-5 column (5% diphenyl-polysiloxane, 95% dimethyl) is commonly used for separation of PAHs (Mosi, 1998). A carrier gas, commonly helium, is used as the mobile phase (providing force to push/pull the analytes down the column).

When a sample volume, ΔV , is introduced into a column some of it stays in the mobile phase, m , while the rest partitions onto the stationary phase, s , shown in

figure 6. The amount that stays in the gas phase relative to the amount in the stationary phase in one time step defines the distribution/partition coefficient, K and is expressed in equation 1:

$$K = \frac{C_s}{C_m} \text{ eq'n 1}$$

In the next time step some of the compounds in the stationary phase will stay on the stationary phase while the rest will enter the mobile phase as defined by K . The analyte originally in the mobile phase has been carried on partitioning between the two phases. Large values of K , indicate preferential portioning onto the stationary phase while small values of K indicate the analyte moves quickly down the column.

The time from when an analyte enters the column to the time it exits the column is defined as the retention time, t_r . Similarly the retention volume, V_r , is the volume of mobile phase (carrier gas) that passes through the column until the analyte exits at a given flow rate, f . The relation between flow rate, retention volume and retention time is shown in equation 2.

$$V_r = t_r f \text{ eq'n 2}$$

The capacity factor of a column is given by equation 3, where adjusted retention times or retention volumes adjusted to compensate for the time it takes for a carrier gas to elute are used.

$$k = \frac{t_r}{t_m} = \frac{V_r}{V_m} \text{ eq'n 3}$$

To compare retention times/volumes of an analyte on different instruments relative retention volumes, V_{rr} , given in equation 4, are used to compensate for different experimental conditions. Retention volumes relative to a standard are found: $V_{r,a}$ -analyte retention volume, V_m -retention volume of carrier, $V_{R,s}$ -retention volume of standard.

$$V_{rr} = \frac{V_{R,a} - V_m}{V_{R,s} - V_m} \text{ eq'n 4}$$

Peak resolution, R , is a measure of separation of compounds is given in equation 5, as the difference in retention times of two neighbouring peaks divided half the sum of the width of each peak. The larger the value of R the greater the separation. Assuming a Gaussian distribution an R value equal to 1.5 means overlap of only 0.13% (Berezkin, 1991)

$$R = \frac{t_{r,B} - t_{r,A}}{0.5(w_B + w_A)} \text{ eq'n 5}$$

When an analyte is first introduced onto the column it occupies a small volume of space, as it travels the volume increases shown in figure 5. The increase in volume results in peak broadening and is one reason why chromatographic peaks are not sharp lines. Borrowed from distillation, the model of theoretical plates can be used to describe chromatographic column efficiency. The column can be thought as being made up of theoretical plates, each plate a discrete length. The number of theoretical plates is found by dividing the length of the column, L , by the plate height, H , as shown in equation 6. The greater the number of theoretical plates (the smaller the plate height) the more efficient the column and the less peak broadening.

$$N = \frac{L}{H} \text{ eq'n 6}$$

Peak broadening can be measured by the variance or standard deviation of the peak, assuming a Gaussian distribution. The height of a theoretical plate is defined in equation 7 as the variance, σ^2 , with respect to column length.

$$H = \frac{\sigma^2}{L} \text{ eq'n 7}$$

The number of theoretical plates can be estimated by equation 8 from the width at half height:

$$N = 5.545 \left(\frac{t_r}{w_{1/2}} \right)^2 \text{ eq'n 8}$$

1.3.4 Tailing/Fronting of Chromatographic Peaks

A chromatographic peak should be symmetrical if the partition co-efficients are equal down the column as shown in figure 3a. Fronting of peaks can happen when the column is overloaded with too much sample, shown in figure 3b. Tailing happens when the analyte sticks to some sites on the stationary phase more than others, shown in figure 3c.

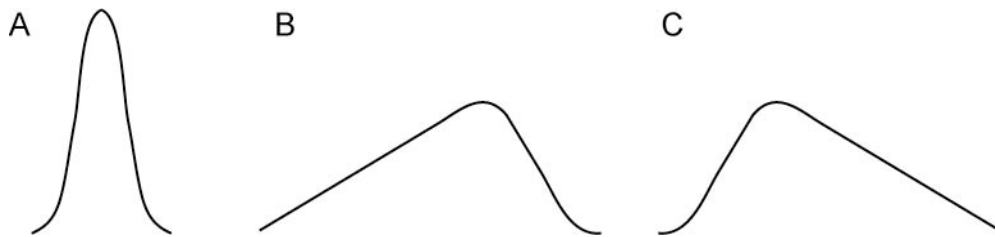


Figure 3: Various Chromatographic Peak Shapes

1.3.5 Peak Broadening of Chromatographic Peaks

Peak broadening can be due to several factors. Three general mechanisms are described below:

The analyte can take any one of multiple paths through the column. By random variation in the path taken, the distance traveled varies. Two possible paths an analyte may take through a column are shown in figure 4.

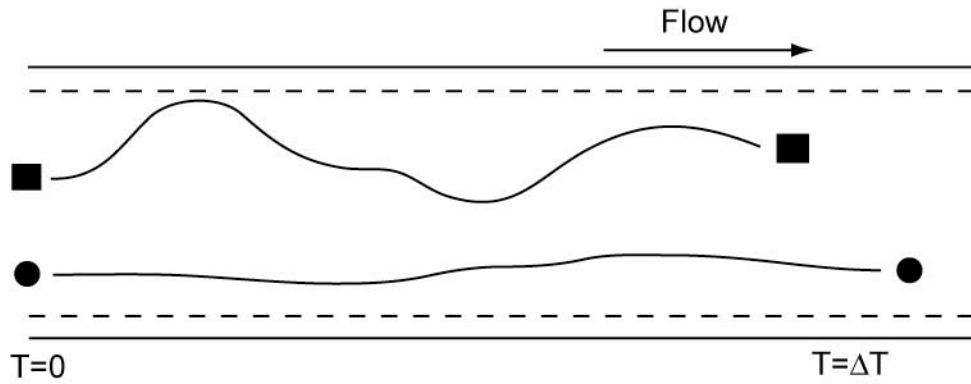


Figure 4: Peak Broadening due to Multiple Paths

Peak broadening can also rise from longitudinal diffusion of analyte molecules.

Figure 5 shows how chromatographic peak shape is affected by analyte diffusion from areas of high concentration to areas of lower concentration.

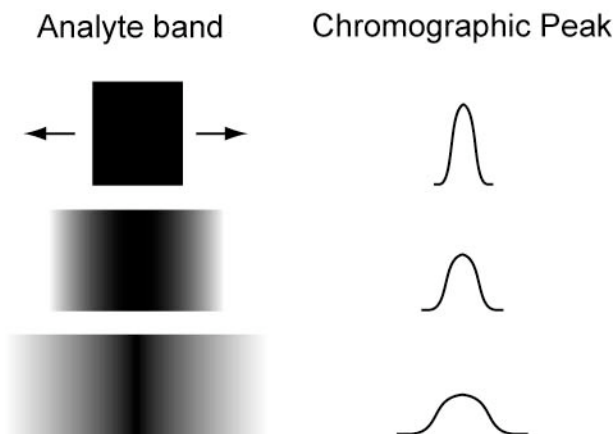


Figure 5: Peak Broadening due to Longitudinal Diffusion

Peak broadening can also occur from delay in time for mass transfer from the stationary phase, s , to the mobile phase, m . Figure 6 shows analyte diffusion over several time steps. Initially the analyte is in a narrowly defined band. With time some analyte will interact with the stationary phase while the rest moves forward. At the second interval some of the analyte that originally interacted with

the stationary phase will re-enter the mobile phase while some will stay on the column. Analyte in other regions will also either interact with the mobile phase or by stationary. Over time the analyte spreads out over a zone.

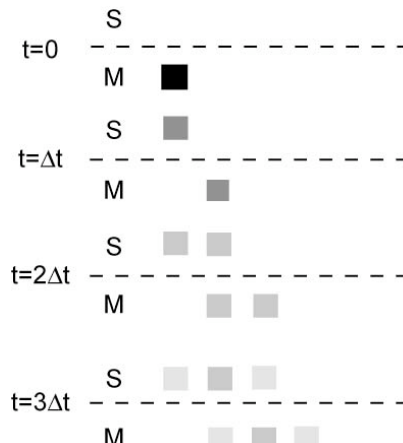


Figure 6: Peak Broadening due to Mass Transfer

1.3.6 van Deemter Equation

The van Deemter equation, equation 9, relates the number of theoretical plates, H , to the three parameters previously discussed: Multiple paths, A , longitudinal diffusion, B/μ and analyte mass transfer, $C\mu$.

$$H = A + \frac{B}{\mu} + C\mu \quad \text{eq'n 9}$$

1.3.7 Mass Spectrometry

Separation of masses can be achieved through a variety of techniques. Mass spectrometers are powerful qualitative and quantitative tools. Initially samples are ionized either by bombardment of high-energy electrons or chemically. The ionized molecules are then sorted by their mass to charge ratio.

1.3.8 Ion-Trap Mass Spectrometer

An ion-trap mass spectrometer, shown in figure 7, can easily be interfaced with a GC and is fairly compact. Eluent enters a chamber where it is ionized by electron impact. The ions are trapped in the chamber and held in stable trajectories by oscillating radio frequencies. Ions of specific mass to charge ratio are allowed to exit to the detector, when radio frequencies are applied to the end plates.

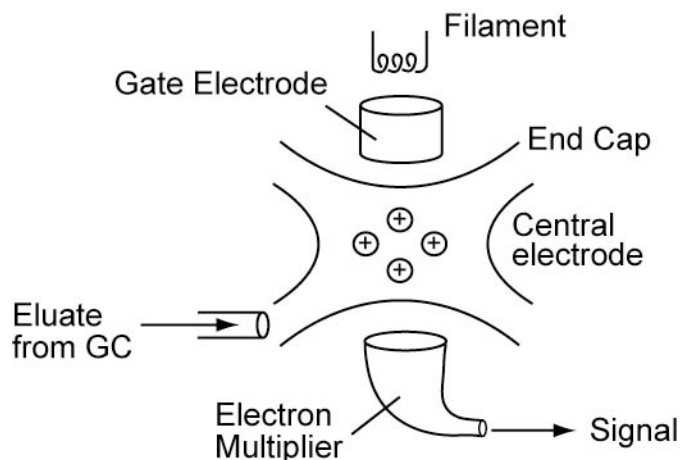


Figure 7: Ion-Trap Mass Spectrometer
(Adopted from Harris, 1999)

1.3.9 Mass Spectra

A mass spectra shows the relative abundances of the various masses. A molecular ion, M^+ , representing the singly charged analyte ion will often be seen with a mass equivalent to the molecular mass of the most common isotope. Isotope clustering can be seen in compounds that contain chlorine or other elements that have naturally occurring isotopes.

Due to the high energy of the electrons used to bombard the sample, compounds often break up into fragments. Daughter ions or pieces of the original compound are also seen in the spectra. The way in which a molecule breaks can be used to identify it. Fragmentation patterns are formed when molecules break-up in stable chunks. When the fragments are energetically more stable than the parent molecule the molecular peak may be dwarfed by fragment peaks. A computerized library search to identify a compound matches up the distinctive fragmentation pattern of a sample to a library of known patterns.

2. Experimental

2.1 Sample Collection

Sediment samples were collected by a large field team September 24 & Oct 1 2004 under special permit obtained by Michael F.J. Pisaric (Department of Geography and Environmental Studies) Research Permit # 2704 NCC File A7170-2704.

A collapsible boat and portable raft, shown in plate 2, were used as platforms on the lake. A dual frequency sub-bottom profiler (Knudson Engineering Limited 320 B/P echosounder), fishfinder (Eagle Ultra), YSI oxygen, conductivity, salinity, temperature meter were used to collect data on Pink Lake. Sediment samples were collected by an Eckman Grab, modified Livingston corer, and a freeze box core.



Plate 2: Photographs of Sample Collection

The freeze corer was filled with a slurry of dry ice nuggets mixed with isopropanol. The freeze corer was lowered through the water column via 20 m of drill rods and sat for 20 minutes. The freeze core was recovered via a hand crank, brought back to shore where the top layer was scrapped off, washed with lake water, lifted from the box corer and placed on wooden boards wrapped in aluminum foil and saran wrap. The core was cooled in coolers until being stored in a freezer at Carleton University at -8°C .

2.2 X-Ray/Lead Analysis

The core, shown in plate 3a, was x-rayed at Alta Vista Animal Hospital XMA (xray Marketing Association) Model A300, 300 Milliamperes at 125 kvp.

The frozen core was sub-sampled every 0.5 cm for the top 55 cm using a Kyocera ceramic knife, plate 3B. Equal amounts of sediment was collected for ^{210}Pb dating, diatom microorganism analysis and for PAH analysis. Lead and PAH samples were stored at -4°C until use, diatom samples were stored at 4°C .

Plate 1c shows samples that were dried to constant weight (36-48 hrs), as measured on a Sartorius BP121S analytical balance, in a Labline oven with temperature no higher than 50°C . Samples were ground to a fine powder with a mortar and pestle as shown in plate 3d.

Samples were sent to MyCore Scientific Inc of Dunrobin, Ontario for ^{210}Pb analysis.

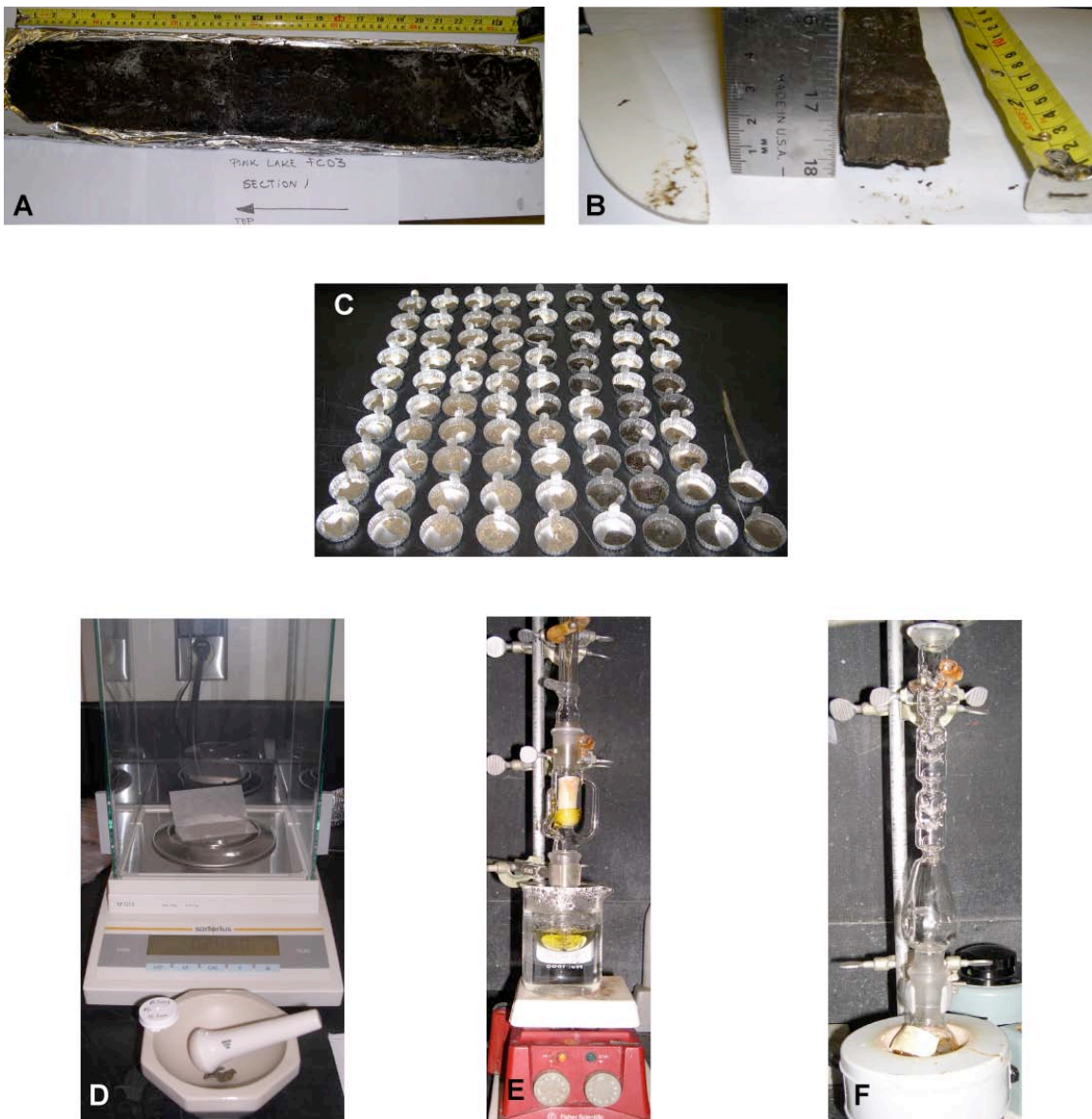


Plate 3: Photographs of Stages of Processing

2.3 PAH Analysis:

Samples were sonicated in a Bronson sonicator for 6 hrs in 4-5 mL of methanol in 14 mL Teflon topped vials. The methanol was decanted off, the original sediment and vials were washed 3 times with 1.5 mL of methanol. Analysis of the first 15 extracts and 10 other extracts spanning the length of the freeze core was

carried out. The extracts were passed through florisil columns until the color of the last of the column was unchanged, typically 4-6 columns. Florisil columns were made by packing florisil in a Pasteur pipet between 8-micron Pyrex fibre glass plugs. The florisil columns were approximately 7 cm long. Alumina columns were prepared by baking alumina (aluminum oxide) from M. Woelm of Germany at 425°C in a Temco oven for 14 hrs. Mel of distilled water was added to 50 g of alumina powder to produce alumina of activity level 4.

PAH stock standard solutions of 100 ppm were made in methanol from pure solid of naphthalene, anthracene, benzanthracene and chrysene. Solutions of 1,2,4,10, 100 ppb and 1 ppm were made by serial dilution.

A PAH standard (EPA 610 polynuclear aromatic hydrocarbons mix 100-2000mg/mL in 1:1 methanol & CH₂Cl₂ lot number LB20875) was obtained from Supelco of Bellefonte, PA. The 1 mL PAH standard was diluted by a factor of 100 with methanol.

The extracts were examined by a Saturn 3400 GC with a Varian Saturn II MS operating in SIM mode, shown schematically in figure 8. The gas chromatograph was fitted with a 29 m DB-5 column with helium carrier gas. Peak integration for all peaks was done manually.

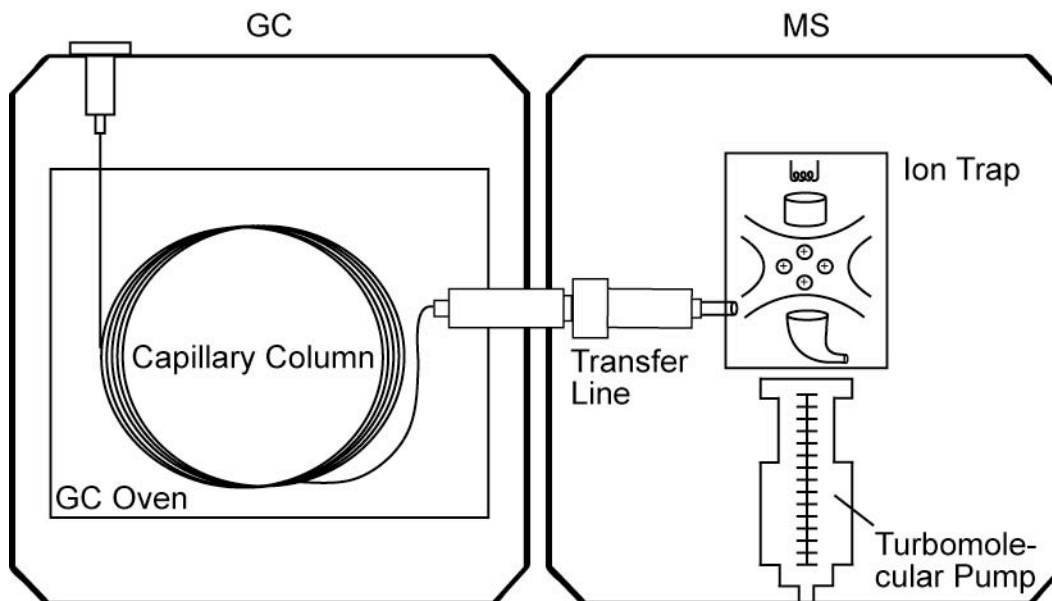


Figure 8: Schematic of Varian Saturn II GC-MS

Glass wool, filter paper, glass frit (fine) and centrifuging (Labnet Hermle Z200A) were tested to remove suspended particulate. Samples were shaken on a Burrell wrist action shaker 75.

Extraction tests were done with a Soxhlet extractor, pictured on plate 1e and shown schematically in figure 9. Cellulose 16 mm x 45 mm Whatman thimbles were used. A Kuderna-Danish concentrator shown on plate 1f, was used to concentrate extracts to 3 mL, after which a stream of nitrogen gas was used to further concentrate extracts to 1 mL.

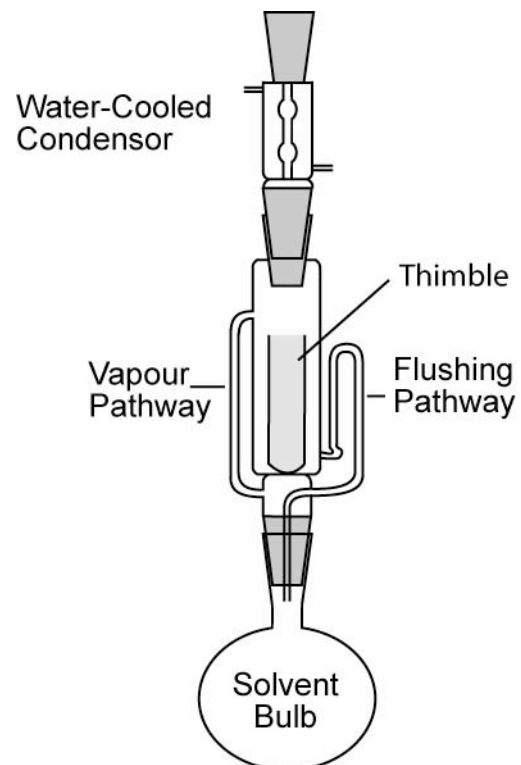


Figure 9: Soxhlet Apparatus

3 Results and Discussion:

3.1 PAH analysis of Pink Lake Sediment

Analysis of sediment determined individual PAH concentrations to be less than 1 part per billion (ppb) dry weight w/w. Chromatograms of concentrated extracts from sediment samples taken every 0.5 cm showed no PAHs. Even when 15 samples representing 10 cm of the top of the core from approximately 1.0 g of sediment were combined and concentrated to 1.0 mL no PAHs were seen. Given the instrumental detection limits of many of the PAHs was approximately 1 ppb (picogram/microlitre) and that 1.0 μ L was injected, PAH levels were lower than 1 ng/mL or 1 ng/g (ppb) dry sample weight. When the 95% water content is considered PAH levels of the original wet sediment was found to be less than 0.05 ng/g (ppb) in the original wet sediment.

3.2 GC Temperature Programming

Using the PAH standard GC parameters were optimized. Six GC oven programs tested, with subtle differences are given in table 2. Program 6 evolved to provide the best separation of 13 of the 16 PAHs in the PAH standard mixture while minimizing run time. A column heating rate of 10°C/min was found to separate PAHs without increasing run time significantly.

Parameter	Prgm 1	Prgm 2	Prgm 3	Prgm 4	Prgm 5	Prgm 6
Initial Col. Temp.	100°C	100°C	100°C	100°C	150°C	100°C
Initial Col. Temp. Hold time	4.00 min	4.00 min	4.00 min	1.00 min	1.00 min	0 min
Final Col. Temp.	300°C	250°C	300°C	300°C	300°C	300°C
Ramp	15°C/min	10°C/min	15°C/min	15°C/min	12.5°C/min	10°C/min
Column Hold Time	7.00 min	7.00 min	7.00 min	5.00 min	5.00 min	12 min
Initial Injector Temp	300°C	300°C	300°C	300°C	300°C	280°C
Transfer Line	120°C	120°C	120°C	200°C	280°C	280°C
Run time	24.3 min	26 min	24.3 min	19.33 min	18.00 min	32.00 min

Table 2: GC Temperature Programs for PAH Analysis

The final column temperature was varied in an effort to limit column bleed.

Column bleed was seen in the portions of the chromatograms corresponding to higher temperatures. Figure 10 shows chromatogram and mass spectra of no injection runs. The peaks were thought to be caused by the column wall vapourizing and entering the detector. The mass spectra, inset, support this conclusion, is characterized by a large number of masses.

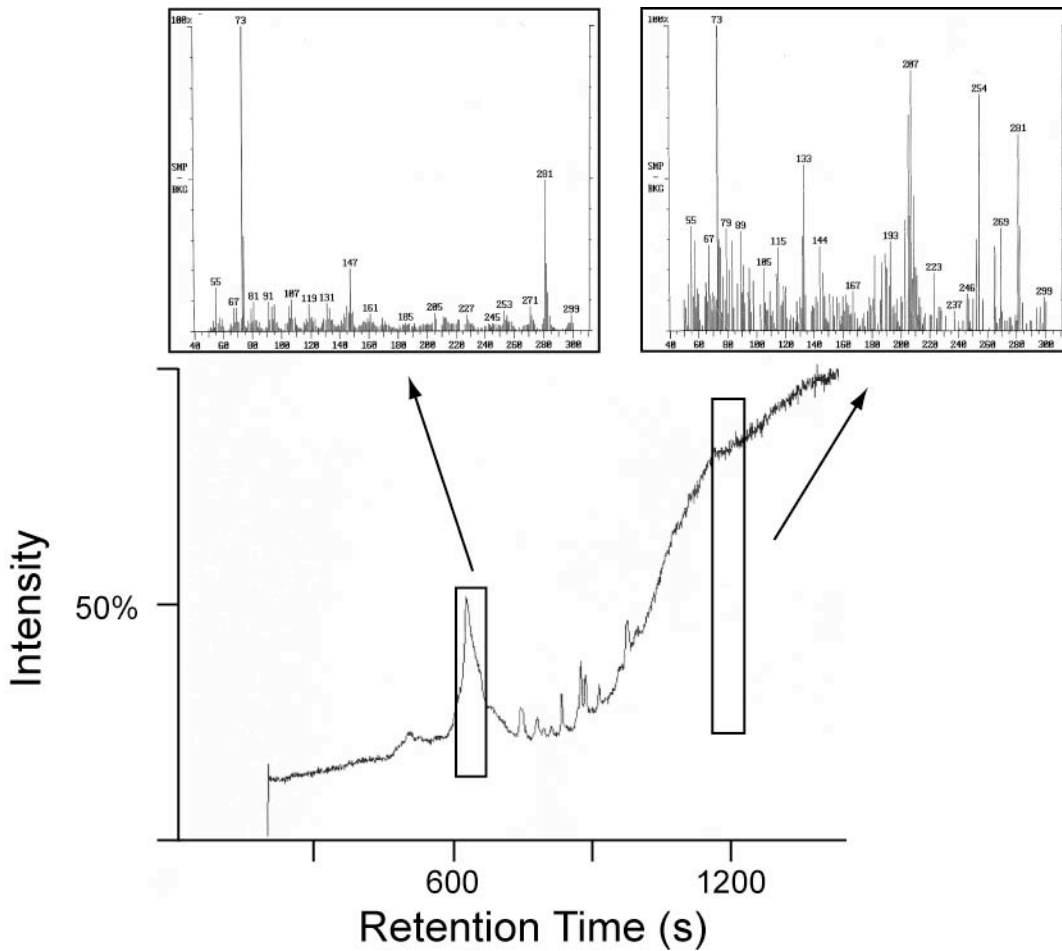


Figure 10: Chromatogram and Mass Spectra of No Injection

Figure 11 shows the effect of column bleed was not significant at higher analyte concentrations, but became significant at lower levels. The column bleed at 100 ppm was found not to be significant however, at lower anthracene levels the chromatogram is defined by the significant signal of column bleed.

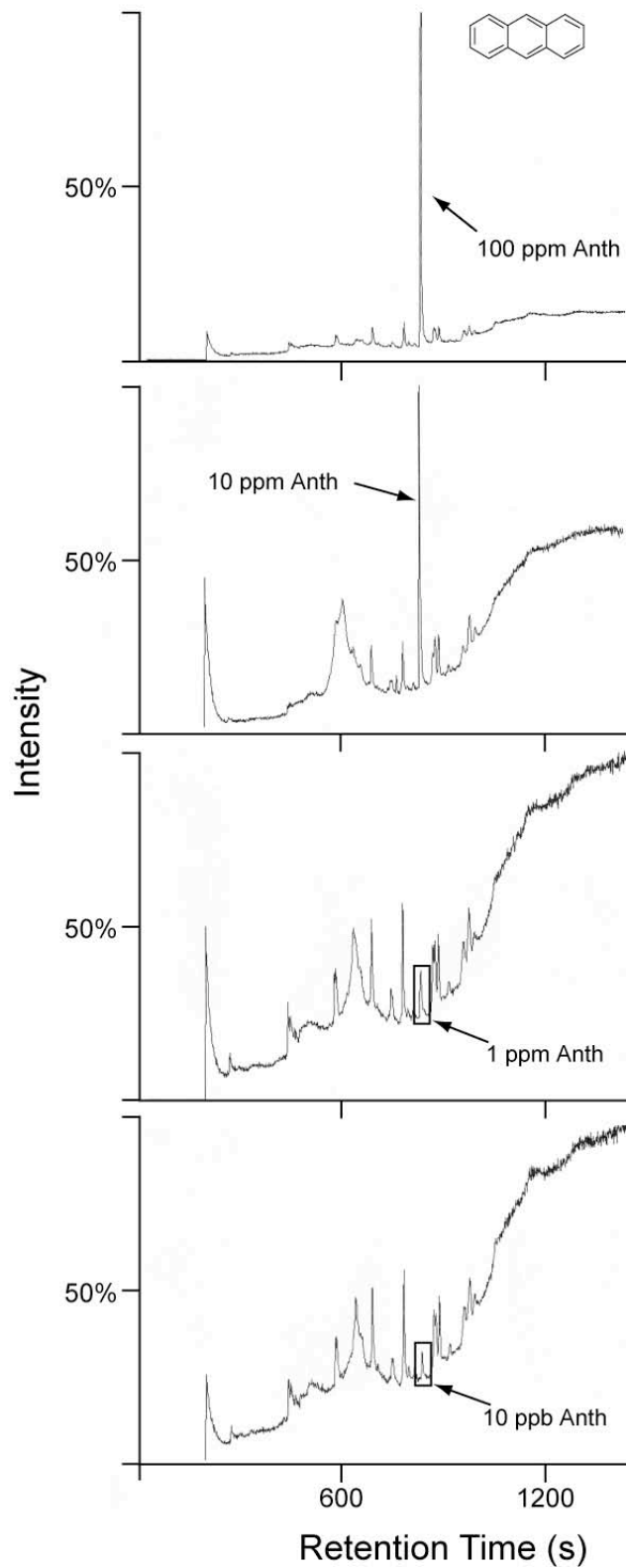


Figure 11: Increasing Column Bleed Effect with Decrease in Analyte Concentration

For later eluting PAHs the signal from column bleed can be a significant interferent making peak area integration difficult. Figure 12 shows peaks due to benzantracene and chrysene eluting as the column bleed occurs. It was found that benzantracene and chrysene elute at the same time making individual quantification difficult.

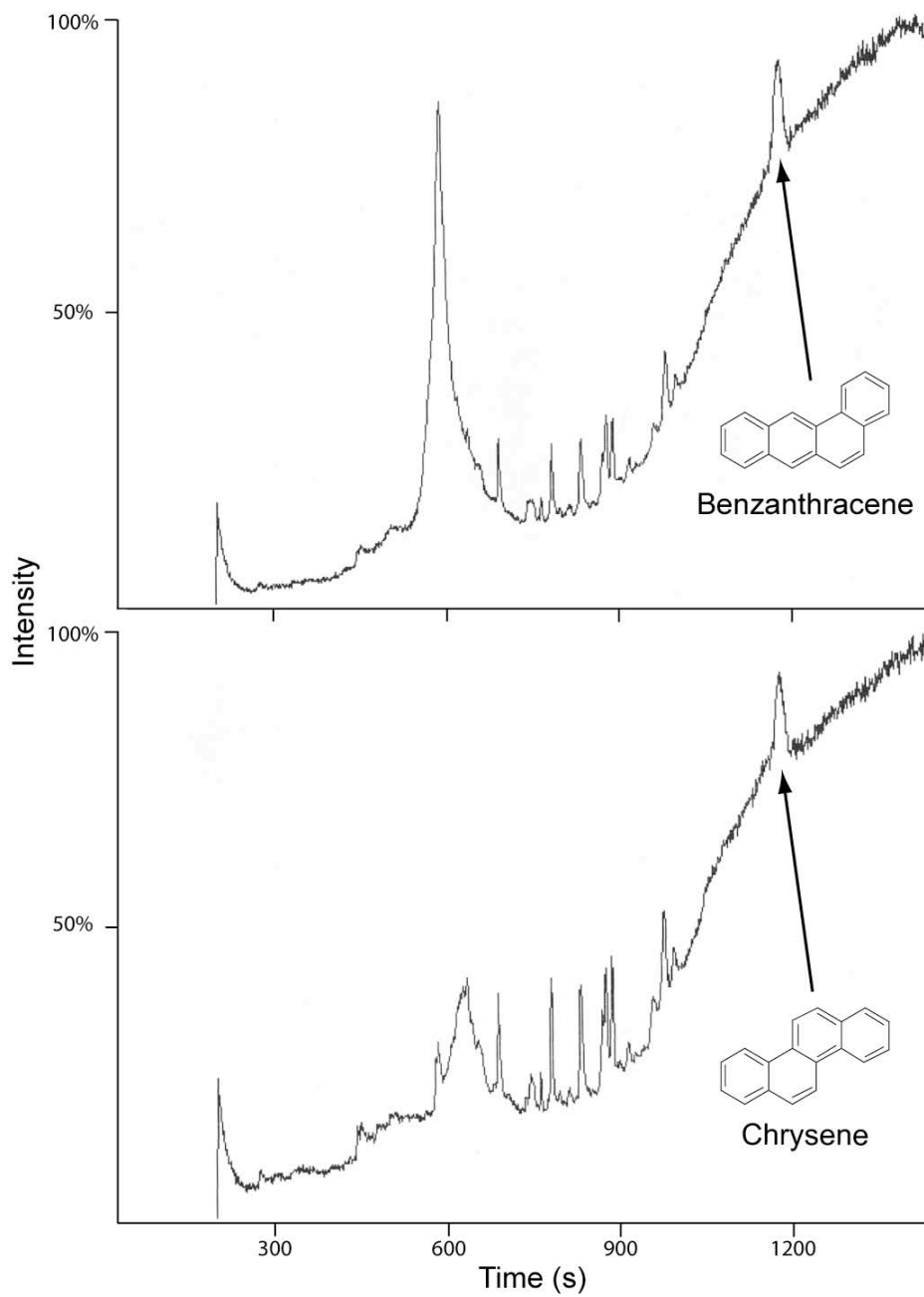


Figure 12: Interference of Column Bleed on Later Eluting PAHs

3.3 Mass Spectrometry

A SIM program was developed to take advantage of the lower detection limits offered by SIM. The elution time of PAHs were found by running PAH standard mixtures on SIM mode for the eight discrete mass ranges. An eight-step SIM program was developed to scan small mass ranges at assigned elution times. The detector was turned on average of 30 seconds before the expected peak and turned off 30 seconds after the expected peak. To reduce the numbers of program steps, solvent delays were used to turn the detector off rather than an additional step. Table 3 gives the 8-step program used to identify 13 of the 16 PAH in the standard down to levels of 1 ppb. Figure 13 shows the separation of 13 of 16 PAHs in the standard mixture.

Step	Time (min.)	Solvent Delay (min.)	Mass Range
1	0-6.3	3.0	126-130
2	6.3-10.0	1.7	150-156
3	10.0-11.5	0.0	164-168
4	11.5-14.1	0.6	176-180
5	14.1-17.1	1.0	200-204
6	17.1-20.7	1.3	226-230
7	20.7-25.0	1.0	250-254
8	25.0-32.0	1.5	274-280

Table 3: SIM Program for PAH Analysis

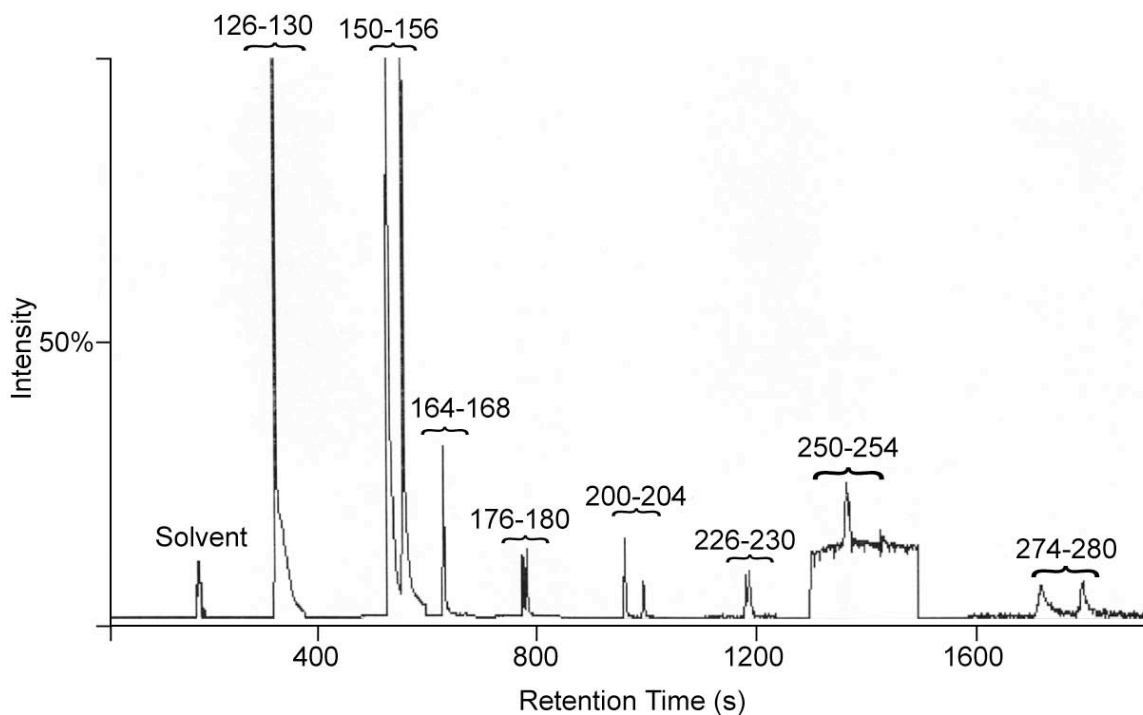


Figure 13: Chromatogram of PAH Mixture Obtained using SIM Program

The mass spectra of each PAH isolated was found to have characteristic fragmentation pattern common to many PAHs. Mass spectra from naphthalene, anthracene and chrysene are shown in figure 14. The stability of the molecules can be seen by the minimal fragmentation even after electron ionization. Some compounds, like chrysene, consistently displayed an M+1 peak rather than a molecular peak.

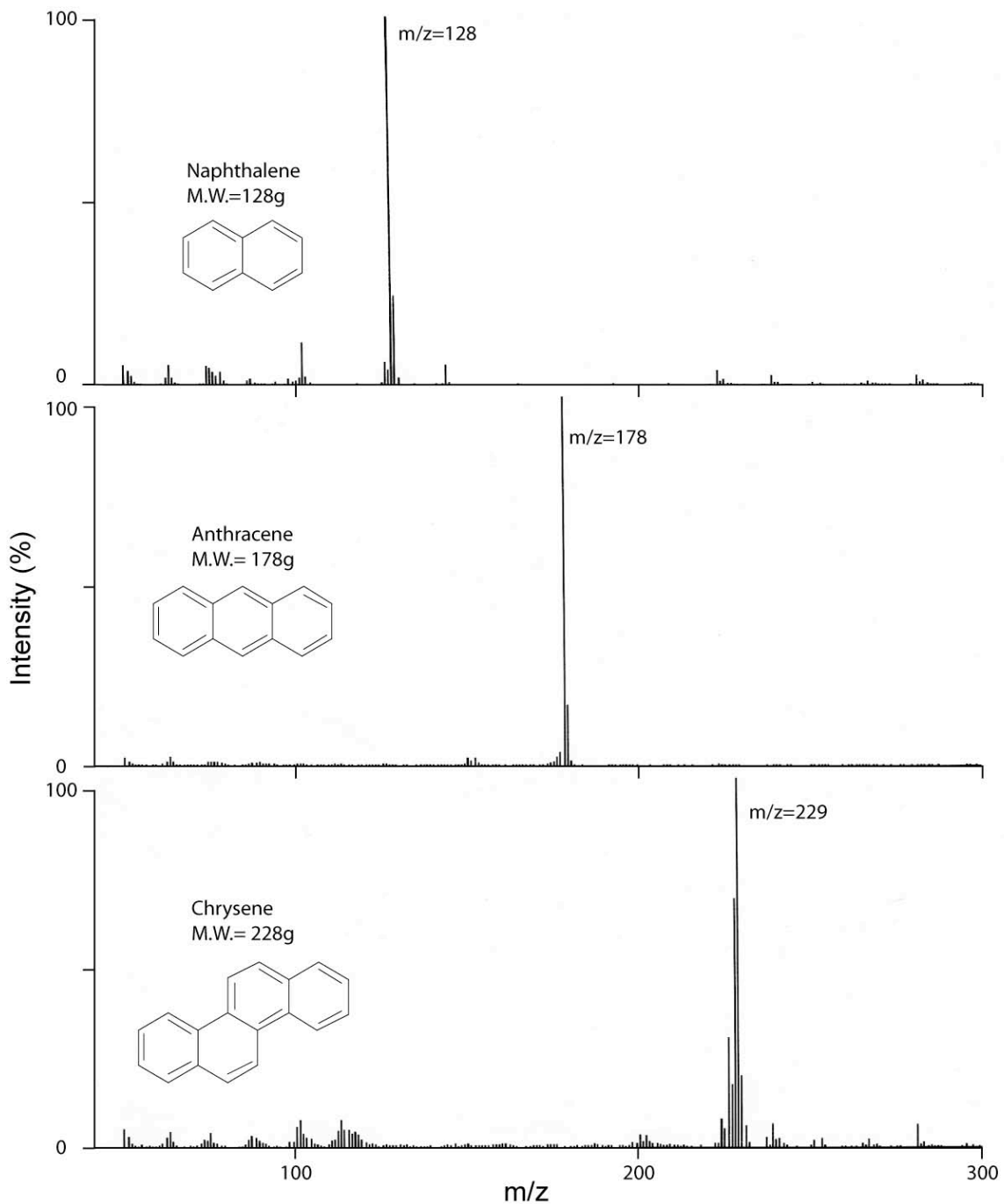


Figure 14: Mass Spectra of Selected PAHs

Analytical calibration curves were constructed plotting instrument response to analyte concentration. Figure 15 shows a calibration curve for anthracene ranging from 1 ppb to 10 ppb. At part per billion levels the linear dynamic range

was only one order of magnitude as instrument response from 100 ppb did not follow the linear curve.

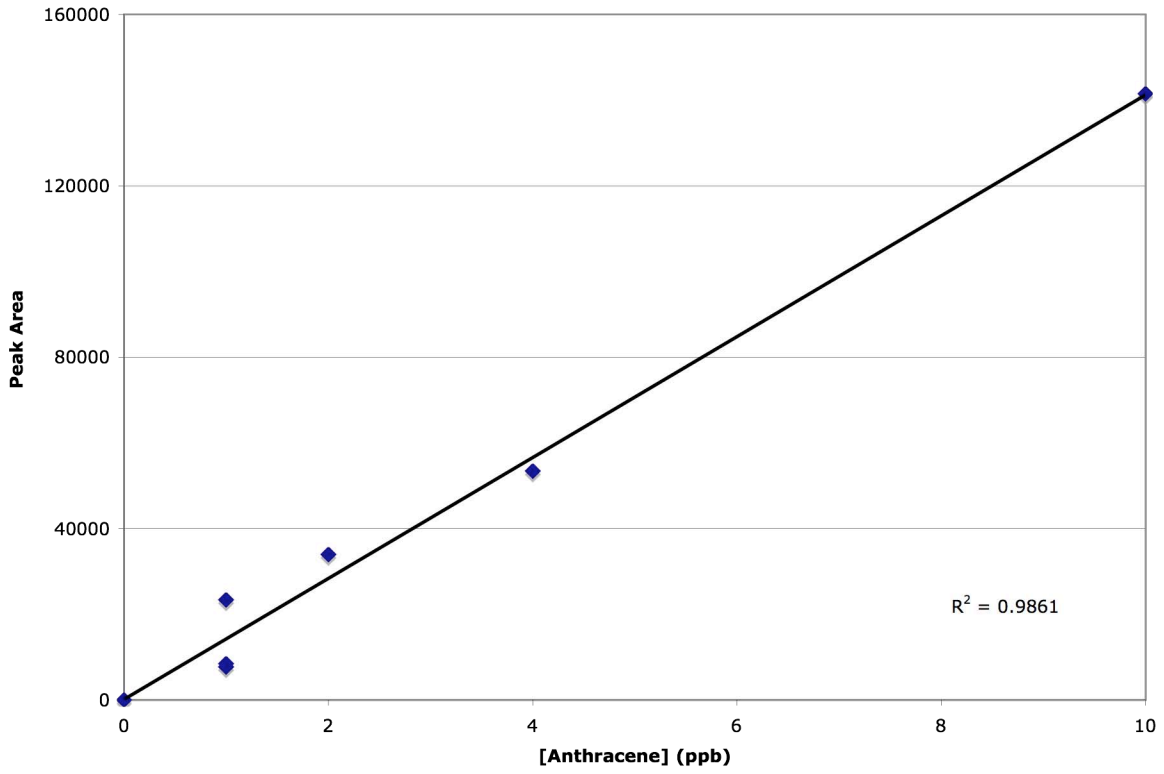


Figure 15: Anthracene Analytical Calibration Curve

3.4 Sediment Extracts

Three techniques: sonication, Soxhlet and shaking, were examined for extraction of spiked PAHs from sediment. Slight differences in the extracts were found. Of the three the samples those that had been sonicated had the finest suspended particles that didn't settle out after 36 hours. Those samples that had been extracted by Soxhlet extraction had fewer fine particles that did settle out after 24 hours. The samples that had been shaken settled quickly (6-9 hours) to reveal a clear liquid on the surface. A wide variety of colors were observed in the extracts as shown in figure 16. The original sediment is shown on the far left. The first four vials show the extracts from the Soxhlet, two orange extracts (vials 6,8 & 9) are from sonication. The rest, 11-19, are from sonication of unspiked freeze core samples. The difference in yellow color is due to dilution of some samples.

A variety of color was observed in the cellulose Soxhlet thimble, filter paper and cleanup columns. After extractions Soxhlet thimbles had a red-orange tint. Filter paper for Soxhlet and sonication samples was reddish. No significant color difference in florisil and alumina columns was observed. Both column types displayed a range of colors after extracts were passed through them: reds, yellows and browns.



Figure 16: Variety of Colors from Extracts

Figure 17 shows the dark color of the first extract in a Soxhlet extraction. The color of initial extracts was a deep yellow-brown, but the condensing methanol was clear indicating that higher boiling point compounds were accumulating in the solvent bulb. After 3-4 hours the extract flushing into the solvent bulb was as clear as the original methanol indicating all the extractables had been extracted.

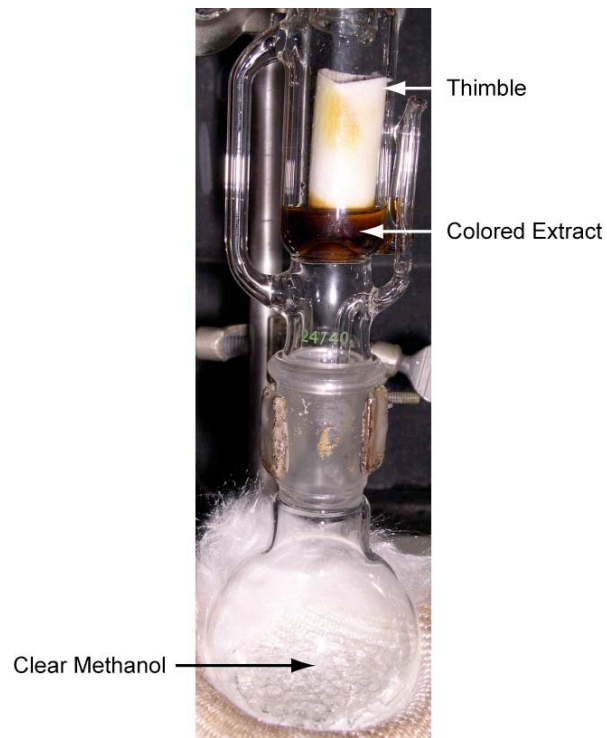


Figure 17: Analyte Extraction into Methanol via a Soxhlet

Figure 18 shows the original sediment, dried sediment, methanol extract and cleaned up extract. The degree of clean up achieved from the florisil column and centrifugation is apparent.



Figure 18: Photo of Samples at Different Stage of Analysis

3.5 Sample Clean Up

After extraction and concentration by a Kuderna-Danish concentrator samples required extensive clean up. The most efficient combination clean up procedure was found to be through several florisil columns and centrifuged for 20 minutes at 5800 rpm. Extracts were passed through florisil columns until the columns were clear. Fine filter paper was not as effective as a fine glass frit in removing fine suspended particles. Even after several columns the extracts were still colored a bright yellow. The yellow component of the extract was not identified. It did not appear in total ion chromatograms of the extracts.

Florisil was found to be as effective at removing some colored portions of the extracts as alumina (activity grade IV).

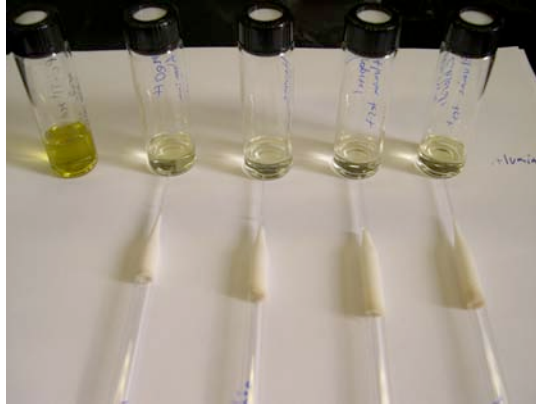


Figure 19: Extract Clean Up via Florisil Columns

In qualitative tests solvent polarity was found not to affect PAH elution from both florisil and alumina columns. Four solvents ranging in polarity from hexane to methanol were tested. Each of the four solvents tested: methanol, hexane, methylene chloride and 2-propanol eluted sediment extracts spiked with PAH standards. Peaks due to the spiked PAHs are clearly evident in figure 20. It was expected that PAHs, that are generally non-polar, would not be eluted to the same degree by polar methanol as non-polar hexane.

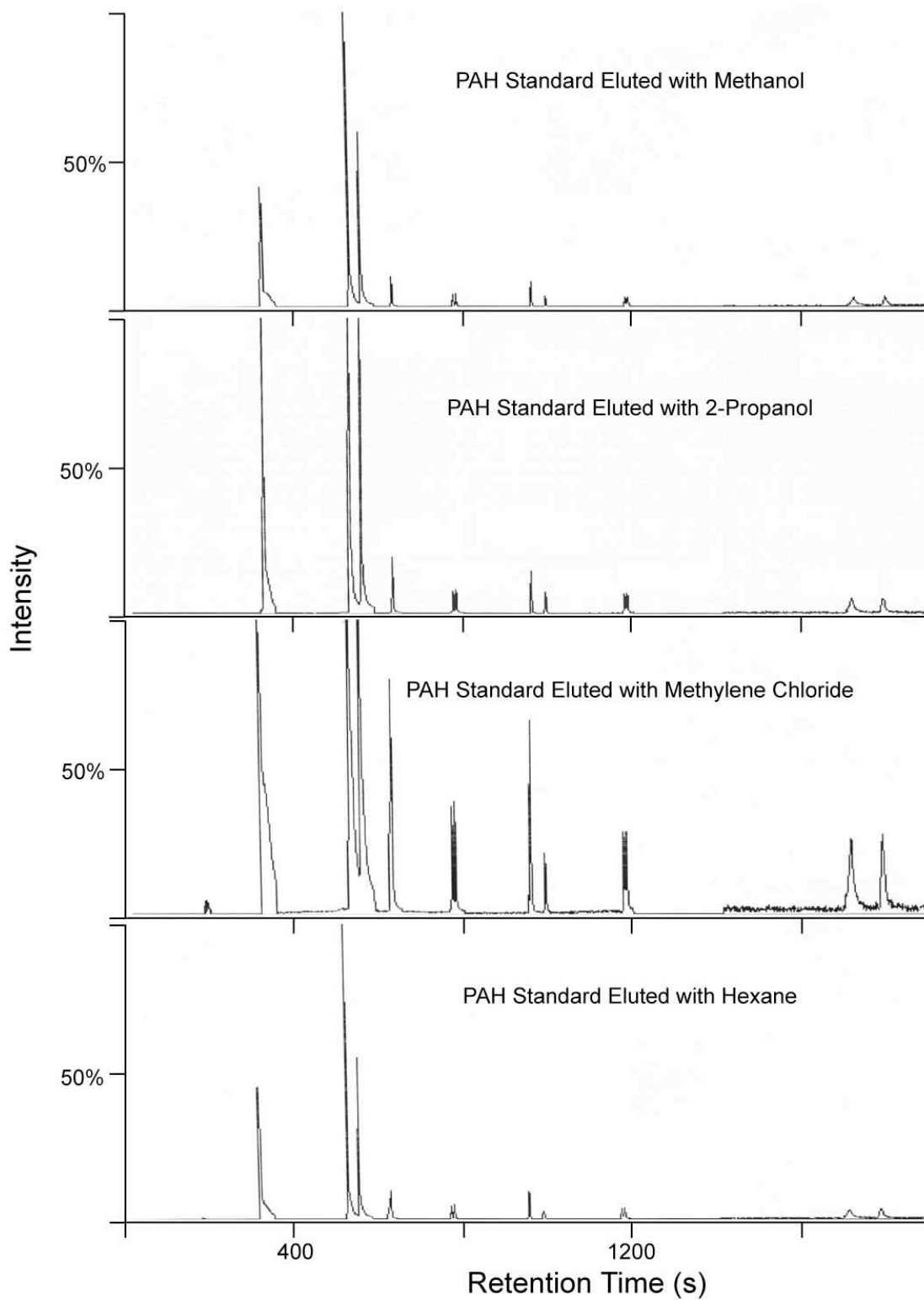


Figure 20: Chromatograms of Spiked Sediment Extracts Eluted from Florisil Columns with Solvents of Differing Polarity

3.6 Pink Lake

Water content was found to be consistent at 94% w/w. Water content was found to decrease slightly from 94.4 % w/w in the top 20 cm to 93.6 % w/w in the bottom 15 cm. It is expected some dewatering occurs with increased pressure down the core.

Freeze Core Depth (cm)	Water Content (% w/w)
0-10	94.0
10-20	94.8
20-30	94.6
30-40	94.1
40-50	93.6
50-55	93.7

Table 4: Water Content of Pink Lake Freeze Core

Pink Lake was found to be meromictic with dissolved oxygen levels dropping to near zero (0.16 mg/L) 12 m below the surface from 8. mg/L at the lake's surface. Figure 21 shows dissolved oxygen variation in relation to water depth. Similarly water temperature dropped from 17°C to 20°C at the surface to 4.5°C at 14 m below the surface as seen in figure 22.

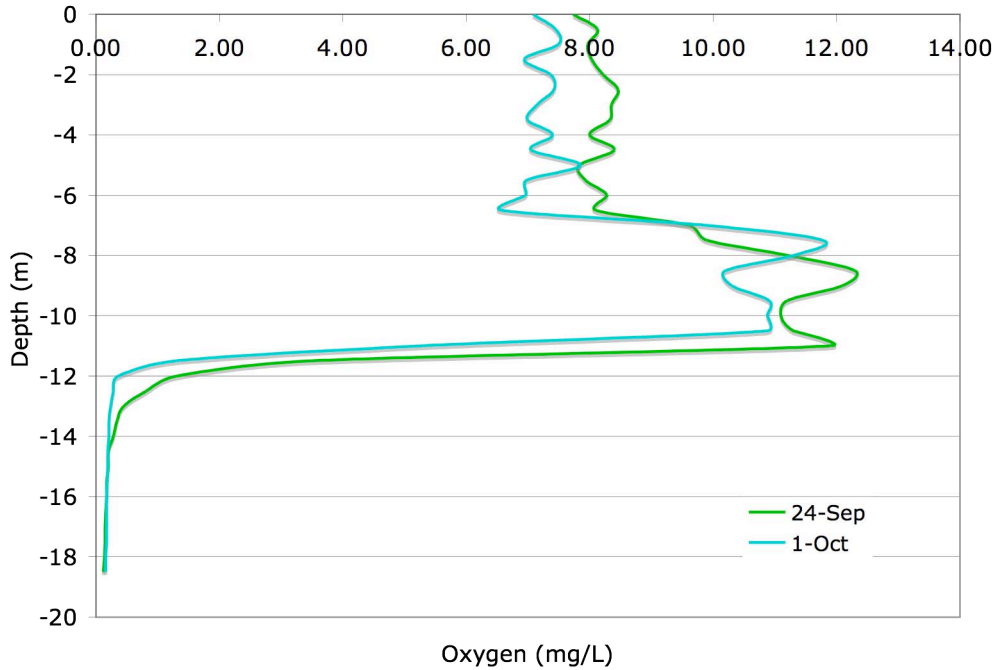


Figure 21: Dependence of Oxygen Levels on Water Depth

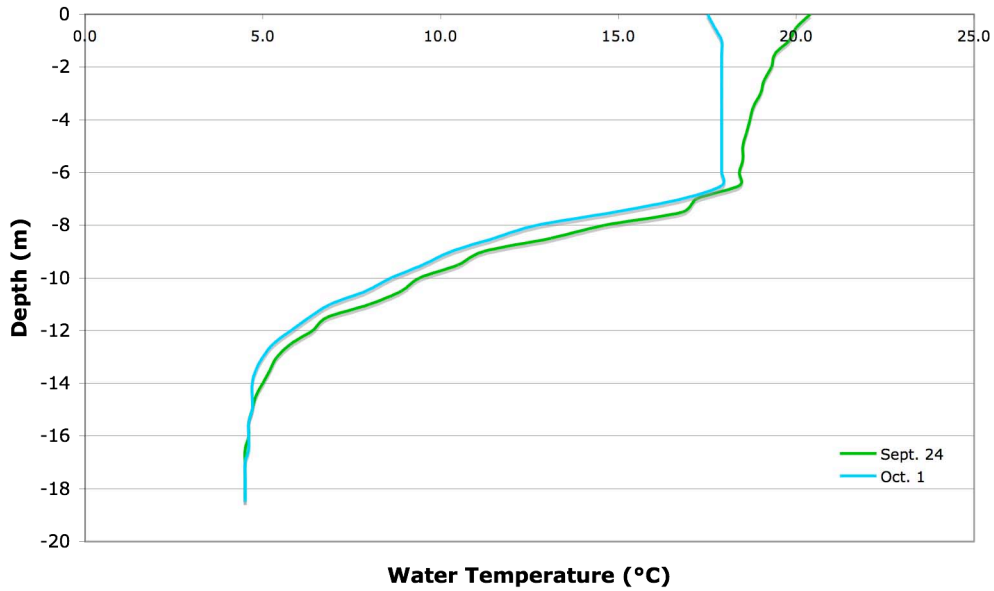


Figure 22: Dependence of Water Temperature on Water Depth

Figure 23 shows a sub-bottom profile from an east to west transect of Pink Lake revealing that the lake is consistently 19-20m in depth. The lake has been previously reported by Dickman and Mott as between 15-18m deep with two

holes at either end 20 and 18 m deep. The original mapping of the lake bottom was done by Boyko in 1973 as part of a Master's thesis at the University of Toronto. The lake bottom has likely not changed significantly over the last 30 years indicating the original mapping was incorrect.

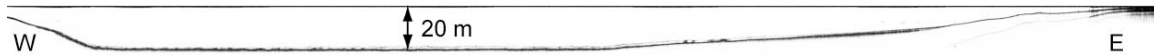


Figure 23: Sub-Bottom Profile of Pink Lake

The lead analysis analysis failed to yield results. Lead levels in the samples could not be differentiated from background levels. The failure of lead analysis may be due to small sample size and low sedimentation rates. Due to its half-life of 22.3 years ²¹⁰Pb analysis can only be used in samples less than 300 years old. Using sedimentation rates established by Jones, 0.39 mm/year, from carbon dating, 11 cm represents 300 years. There was likely too few samples (after some were combined to make up the required mass) from the top 11 cm to construct a lead calibration curve.

The absence of annual lamination in X-rays of the freeze cores was unexpected. The 30 m high cliffs that encircle Pink Lake and 20 m water depth should protect the bottom of the lake from wind disturbance. The lack of oxygen and resultant lack of many organisms should limit sediment mixing. Dickman proposes that iron rich dark sediments do not form owing to a lack of iron and other sulfide forming metals (Dickman, 1978). However this model does not explain the lack of light colored sediment. Metal levels in the lake water could be tested to

determine whether the lake has sufficient levels of iron or whether some unknown cause is responsible for the lack of laminations.

Laminations together with ^{210}Pb dating are commonly used for geochronology of sediment cores. However in the absence of results from either other forms of dating must be found. While ^{13}C is used for samples 1000 years and older, interpolation of sedimentation rates forward can be problematic. Sediments overlying those used for ^{13}C analysis are not subjected to the same degree of compression and dewatering and a linear sedimentation rate cannot be assumed.

3.7 Suitability of PAH as Land-Use change Proxy

Despite levels of PAHs being below detection limits they are potentially powerful proxies for land use-change as natural and anthropogenic sources of PAHs are identifiable by characteristic patterns in levels and alkyl substitution. The fate of air deposited PAHs, whether they migrate through the water column to become incorporated into lake sediments or are sequestered in the food chain, requires further investigation. Further study of PAH soil stratigraphy would likely confirm their usefulness.

4 Conclusions

Further work is needed to improve extraction and cleanup methods in addition to improving the limits of detection for PAH analysis in these sediments. Further research investigating the applicability of lead dating or another geochronology methods on sediments from Pink Lake is needed.

5 References:

Berezkin V.G., Gas-Liquid-Solid Chromatography, Marcel Dekker Inc, 1991, New York

Chemfinder Chemical Database, 2005, <http://chemfinder.cambridgesoft.com/>

Cwynar L., The Recent Fire History of Barron Township, Algonquin Park, Can. J. Bot. 55, 1977, 1524-1538

Dickman M., A possible Varving Mechanism for Meromictic Lakes, Quaternary Research 11, 113-124, 1979

Groß R., Chromatographic Analysis of the Environment, Marcel Dekker Inc, 1975, New York

Harris D., Quantitative Chemical Analysis, Fifth Edition, Freeman, 1999

Jones R., Late Quaternary Diatom and Chemical Profiles from a Meromictic Lake in Quebec Canada, Chemical Geology 44, 1984, 267-286

Kim E., Effects of Forest Fire on the Level and Distribution of PCSS/Fs and PAHs in Soil, The Science of the Total Environment 311, 2003, 177-189

Mosi A., Analysis of Polycyclic Aromatic Hydrocarbons by Chemical Ionization and Ion Trap Mass Spectrometry, University of BC, 1998

Mott R.J. et al., Two Late Quaternary Pollen Profiles from Gatineau Park, Quebec, Canada Geological Survey Paper 80-31, 1981, 1-10

Naraoka et al, Isotopic Evidence from an Antarctic Carbonaceous Chondrite for two Reaction Pathways of Extraterrestrial PAH Formation, Earth and Planetary Science Letters 184, 2000 1-7

National Capital Commission, 2005,
http://www.capcan.ca/gatineau/nature/pinklake_e.asp

Song Y.F., Comparative Study of Extraction Methods for the Determination of PAHs from Contaminated Soils and Sediments, Chemosphere 48, 2002

Wang X, Distribution and Partitioning of Polycyclic Aromatic Hydrocarbons (PAHs) in Different Size Fractions in Sediments from Boston Harbor, United States, Marine Pollution Bulletin Vol 42, Pergamon, 2001, 1139-1149

Wilke W., Polycyclic Aromatic Hydrocarbons (PAHs) in Soil- A Review, J. Plant Nutr. Soil Sci 163, 2000, 229-248

Yunker M., Alkane and PAH Deposition History, sources and Fluxes in Sediments from the Fraser River Basin and Strait of Georgia, Canada, Organic Geochemistry 34, 2003, 1429-1454